

CoMP: Continual Multimodal Pre-training for Vision Foundation Models

Yitong Chen^{1,2*} Lingchen Meng^{1*} Wujian Peng^{1,2} Zuxuan Wu^{1,2†} Yu-Gang Jiang¹

¹Shanghai Key Lab of Intell. Info. Processing, School of CS, Fudan University

²Shanghai Innovation Institute

<https://slimm-x.github.io/comp>

Abstract

Pre-trained Vision Foundation Models (VFs) provide strong visual representations for a wide range of applications. In this paper, we continually pre-train prevailing VFs in a multimodal manner such that they can effortlessly process visual inputs of varying sizes and produce visual representations that are more aligned with language representations, regardless of their original pre-training process. To this end, we introduce CoMP, a carefully designed Continual Multimodal Pre-training pipeline. CoMP uses a Continual Rotary Position Embedding to accommodate visual inputs with different resolutions, and an Alignment Loss between visual and textual features for better cross-modal alignment. After continual pre-training, leading VFs like DINOv2 and SigLIP achieve remarkable improvements not only in multimodal understanding tasks but also in generic classification and segmentation tasks. Remarkably, CoMP-SigLIP achieves scores of 66.7 on ChartQA and 75.9 on DocVQA with a 0.5B LLM, while maintaining an 87.4% accuracy on ImageNet-1K and a 49.5 mIoU on ADE20K under frozen chunk evaluation.

1. Introduction

Pre-training Vision Foundation Models (VFs) capable of extracting transferable representations for various downstream tasks has been a long pursuit of the computer vision community. The key to pre-training is to scale up models and data through constructing strong supervisory signals with weak-strong augmentations in vision-only pre-training [9, 10, 24, 50] or cross-modality alignment in vision-language pre-training [57, 68, 80]. These VFs often demonstrate strong performance for a variety of downstream tasks, and can be easily combined with Large Language Models (LLMs) by designing lightweight adapters

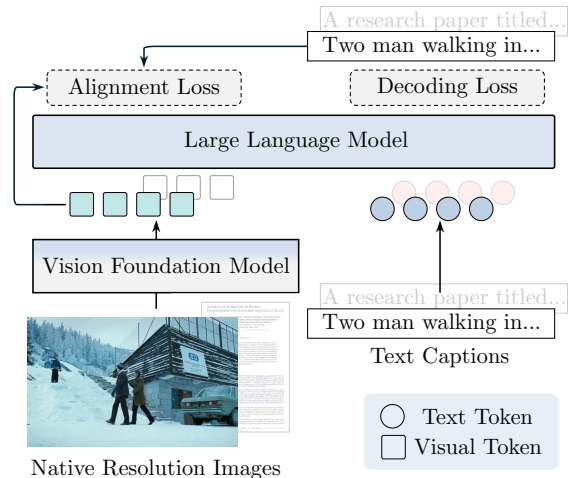


Figure 1. **Overview of CoMP.** Our method accepts an image at native resolution and its corresponding text. Then, in addition to training through text decoding in next-token prediction paradigm, we also explicitly project the visual features into the language space of LLM using Alignment Loss.

that project visual features into text space, serving as the “eyes” of language models.

In this paper, we revisit these widely used VFs such as vision-only pre-training DINOv2 [50] and vision-language pre-training SigLIP [80]. We argue that these prevailing VFs, regardless of their pre-training procedures, can be further boosted through continual multimodal pre-training. This allows VFs to (1) better process visual inputs of arbitrary sizes without requiring resizing, when used as vision encoders of LLMs; (2) produce outputs that are more aligned with language representations, thereby improving multimodal understanding, significantly benefiting encoders from vision-only pre-training.

On one hand, equipping VFs with the ability to deal with images of varying sizes is the core for visual understanding, as image resolutions directly impact the richness of the information within an image. However, existing ap-

* Equal contributions.

† Corresponding author.

proaches treat “an image as worth 16×16 words”[18], resizing all images to a predefined size. This one-size-fits-all strategy results in the loss of critical details, impeding the model’s ability to perceive fine-grained information. This is particularly detrimental in tasks that demand high-resolution inputs, such as chart understanding[46], document parsing [47], and fine-grained recognition [53]. Recent works [7, 50, 64, 68, 80] have attempted to address this challenge by improving bilinear interpolation of positional embeddings and incorporating multi-resolution training. However, they still struggle with real-world scenarios involving diverse input resolutions, as they remain constrained by the limitations of resolution extrapolation.

On the other hand, we believe there is still a representation gap between VFM and LLMs, which results from their distinct training objectives and data modalities during pre-training [37]. To bridge this gap and enable LMMs to better understand visual inputs, the mainstream approach [32, 41, 43] involves training an adapter that projects the visual embeddings of VFM into the textual embedding space of LLMs, typically through next-token prediction for text tokens. However, relying solely on text-based supervision is insufficient to effectively and directly reduce this gap [52], particularly when VFM have not undergone vision-language alignment pretraining [65, 83].

To address these challenges, we introduce COMP, a continual pre-training pipeline that is carefully designed to enhance existing VFM. Specifically, COMP builds upon (1) C-ROPE, a Continual Rotary Position Embedding for vision models, which is operated by adding the standard RoPE-2D [63] with the learned 1D position embedding, to support native resolution continual pre-training; (2) Alignment Loss, a cross-entropy loss between visual and textual features through language prototypes, to align multimodal representations between pre-trained VFM and LMMs.

As shown in Fig. 1, our method accepts an image of native resolution and its corresponding text. Then, in addition to training through next-token prediction on the text, we also explicitly project the visual features into the language space using Alignment Loss by word embedding of LLM. With a three-stage continual pre-training, our models excel not only on multimodal understanding, but also in other downstream tasks such as classification and segmentation. Our contribution can be summarized as:

- We propose a continual multimodal pre-training method COMP, including two techniques, C-ROPE and Alignment Loss, to enable pre-trained VFM supporting native resolution, and aligning representation space of LLM.
- With the COMP, we present COMP-SigLIP and COMP-DINOv2, which achieve remarkable improvements not only in multimodal understanding but also in traditional visual tasks such as classification and segmentation.
- Based on COMP-SigLIP, we introduce COMP-MM-1B

and COMP-MM-7B, which significantly outperforms all other methods under the similar pre-training data size.

- We conduct comprehensive experiments and ablation studies on different models and different tasks, which provide useful insights behind the design choices.

2. Related Work

Vision Foundation Models. Large-scale vision pre-training has achieved remarkable breakthroughs [10, 24, 57, 68, 80], particularly with vision transformers [18] as the backbone, forming the foundation of visual understanding. These pre-training approaches can be broadly categorized into two main directions: vision-only pre-training and vision-language pre-training. In vision-only pre-training, models are trained by either distinguishing image-or patch-level entities from different views using contrastive learning [9, 10, 24, 50] or reconstructing masked patterns back to the raw image [6, 25, 66]. In vision-language pre-training, models are encouraged to align visual and linguistic features into a joint semantic space by leveraging web-scale image-text pairs as the pre-training corpus. In this paper, we explore a continual pre-training paradigm built upon two representative models: DINOv2 [50] for vision-only pre-training and SigLIP [80] for vision-language pre-training. Our approach enhances these models with fine-grained and open-world capabilities beyond image-level pre-training while preserving their original strengths, e.g. image-level classification and pixel-level segmentation.

Large Language Models. Leveraging the strong representational power of Transformers [69], Large Language Models (LLMs) can be pre-trained on large-scale unlabeled text corpora. Specifically, BERT [17] adopts an encoder-decoder architecture and introduces a masked language modeling paradigm, where parts of a sentence are randomly masked and then predicted by the model. This approach has proven effective for representation learning and has demonstrated strong performance on downstream tasks after fine-tuning. Subsequent works [29, 30, 58] further improve the performance through multi-task training and data scaling. Meanwhile, GPT series [8, 55, 56] utilize decoder-only Transformers and optimize under the next-token prediction paradigm with a causal mask, enabling emergent text generation capabilities. Building on this foundation, Instruct-GPT [51] and ChatGPT enhance instruction-following capabilities, making LLMs more suitable for real-world applications. In response to ChatGPT, recent open-source projects such as LLaMA [19, 67], Qwen [3, 76, 77], and DeepSeek [14], have attracted significant attention, driving further advancements in the community. In this paper, we leverage pre-trained LLMs as an interface to process various forms of text supervision by captioning the given image, enhancing vision backbones for diverse scenarios.

Multimodal Pre-training CLIP [57] and its follow-ups [27, 54, 59, 81] demonstrate the effectiveness of aligning vision and language modalities into a unified semantic feature space using paired image-text supervision, showcasing promising capabilities in open-set image-level classification and retrieval. However, this vision-language approach faces challenges when dealing with fine-grained tasks, *e.g.* segmentation and detailed caption [39, 72], due to its holistic representation and resolution. More recently, models like Flamingo [2], CoCa [78], and BLIP [33] introduced a cross-attention mechanism to handle image-grounded captions via image-to-text cross-attention, enabling pre-trained models to generate captions for visual inputs. Additionally, with the rapid advancements in large language models (LLMs), recent works leverage pre-trained LLMs as interfaces alongside pre-trained vision encoders to build powerful large multimodal models capable of addressing complex visual question-answering tasks. BLIP-2 [34] and InstructBLIP [13] utilize the previous cross-attention to deal with visual tokens, while LLaVA [40, 41] series project visual features as a sequence of visual tokens and feed them as inputs of LLM. The follow-up works [4, 11, 22, 38, 43, 49, 70, 71] focus on improving multimodal understanding through image tiling, data scaling, and improved vision token processing. In contrast to these approaches, we focus on improving the foundational visual capabilities through a text-supervised generative pre-training paradigm.

Furthermore, we enhance high-resolution capabilities by incorporating RoPE-2D into visual encoding and introducing an additional training objective to better align vision-language features. As a result, our method demonstrates strong performance in multimodal understanding while also improving traditional vision tasks.

3. Method

Our goal is to empower a pre-trained vision foundation model (VFM) with the ability to process images at their native resolution while aligning its encoder features with the representation space of a pre-trained LLM. To achieve this, as shown in Fig. 2 (a), we propose a continual multimodal pre-training pipeline that improves existing VFMs so that they naturally handle native-resolution inputs using C-Rope (Sec. 3.1) and can better align with language embedding through carefully designed loss functions: the text decoding loss (Sec. 3.2) and the cross-modal alignment loss (Sec. 3.3). These components are integrated into a three-stage training framework (Sec. 3.4), ensuring effective adaptation and alignment.

3.1. Native Resolution Adaptation

Vision encoders often use fixed-size inputs during the pre-training stage, and thus struggle to handle images with vary-

ing resolutions, particularly high-resolution images for fine-grained visual understanding. While training on images of different sizes is a straightforward solution, it is particularly challenging due to the predefined shape of position embeddings in vision transformers. A common approach is to interpolate the original position embeddings in an online manner to accommodate different input resolutions, yet the results are unsatisfactory [7, 64].

Inspired by the success of Rotary Position Embedding (RoPE) that demonstrates strong extrapolation capabilities [67, 75] in NLP, we aim to build upon RoPE to handle a sequence of visual tokens. Unlike previous methods [1, 5, 15, 71] that rely on a single position embedding, we leverage both absolute and relative embeddings to capture richer positional information so as to handle a variety of high-resolution inputs. To best leverage the pre-trained knowledge and ensure a smooth transition from the pre-trained vanilla ViT to arbitrary resolutions, we begin by interpolating absolute positional embeddings and then incorporate RoPE-2D. We refer to this method as C-Rope.

Specifically, as shown in Fig. 2 (b), a 2D image of resolution (H, W) is patchified into $N = HW/P^2$ patches $x_p \in \mathbb{R}^{N \times (P^2 \cdot C)}$, where P denotes the patch size of vision encoder and C indicates the number of image channel. The image encoding processes can be expressed as:

$$\mathbf{z}_0 = [\mathbf{x}_p^1 \mathbf{E}; \mathbf{x}_p^2 \mathbf{E}; \dots; \mathbf{x}_p^N \mathbf{E}] + \text{Int}(\mathbf{E}_{\text{pos}}) \quad (1)$$

$$\mathbf{q}_i, \mathbf{k}_i, \mathbf{v}_i = \text{Proj}_q(\mathbf{z}_i), \text{Proj}_k(\mathbf{z}_i), \text{Proj}_v(\mathbf{z}_i) \quad (2)$$

$$\mathbf{y}_i = \mathbf{z}_i + \text{Proj}_o(\text{Softmax}\left(\frac{(\mathbf{R}\mathbf{q}_i)^\top (\mathbf{R}\mathbf{k}_i)}{c}\right)\mathbf{v}) \quad (3)$$

$$\mathbf{z}_{i+1} = \mathbf{y}_i + \mathcal{FFN}(\mathbf{y}_i) \quad \text{where } i = 0, \dots, L-1 \quad (4)$$

where $\mathbf{E} \in \mathbb{R}^{(P^2 \cdot C) \times D_v}$ and $\mathbf{E}_{\text{pos}} \in \mathbb{R}^{N \times D_v}$ indicate patch embedding and learnable position embedding, D_v indicates the hidden dimension of vision encoder, $\text{Int}(\cdot)$ represents bilinear interpolation, $\text{Proj}(\cdot)$ is the projection layer, $\mathcal{FFN}(\cdot)$ denotes standard feed-forward network, and L denotes the number of encoder layers. In particular, \mathbf{R} in Eq. (3) is the 2D rotary matrix:

$$\mathbf{R}_{x,y} = \begin{pmatrix} \cos x\theta & -\sin x\theta & 0 & 0 \\ \sin x\theta & \cos x\theta & 0 & 0 \\ 0 & 0 & \cos y\theta & -\sin y\theta \\ 0 & 0 & \sin y\theta & \cos y\theta \end{pmatrix}$$

3.2. Text-supervised Generative Pre-training

Text-supervised generative pre-training is widely used in large multimodal models (LMMs). It extends the standard text-only autoregressive next-token prediction framework [8, 55, 56] to visual inputs, mapping visual features into the input layer of a large language model via query-driven cross-attention [2, 13, 35] or projection [41]. In this work, we adopt the projection-based multimodal framework

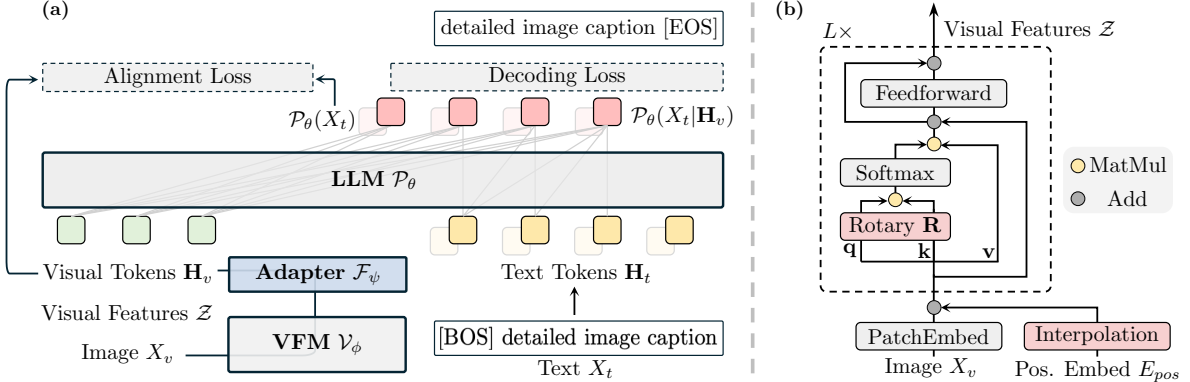


Figure 2. **Architecture of our CoMP.** (a) Overview of our pre-training framework; (b) Detail of C-ROPE. For ease of visualization, the projection layers $\text{Proj}_{q,k,v,o}$ and scale operators are omitted.

due to its simplicity and effectiveness. Formally, the projection procedure \mathcal{F}_ψ can be defined as follows:

$$\mathbf{H}_v = \mathcal{F}_\psi(\mathcal{Z}) \quad (5)$$

where $\mathcal{Z} = \mathbf{z}_L$ in Eq. (4). Then, the image tokens \mathbf{H}_v are fed into the input layer of the LLM \mathcal{P}_θ , serving as the visual condition for the corresponding text X_t . The text decoding loss can then be expressed as:

$$L_{dec} = -\frac{1}{T} \sum_{i=V+1}^{V+T} \log \mathcal{P}_\theta(X_i|X_{<i}, \mathbf{H}_v) \quad (6)$$

where V and T denote the number of visual and textual tokens, respectively. To support the autoregressive generation process, the image-grounded text decoder utilizes causal self-attention mechanisms.

3.3. Vision-language Representation Alignment

Thanks to text-supervised generative pre-training and decoding loss, the vision encoder can be optimized using paired images and texts. However, the supervision is too distant for directly optimizing the vision transformer, especially when the original pre-training of vision encoder does not involve vision-language alignment, such as in image-only SSL of DINOv2 [50] (please refer to the Ablation Sec. 4.5 for the further analysis). To bridge the modality gap between the vision encoder and the language model, we utilize direct vision-language representation alignment by encoding visual and textual features through the vision and text models, respectively.

Inspired by the knowledge distillation in DINO [9, 50], as shown in Fig. 3, we aim to align visual and textual representations by treating the word embeddings \mathbf{W} of the LLM as prototypes [52]. In contrast to the self-distillation approach in DINO, we frame the distillation process as cross-modality text-to-image distillation. Specifically, we first obtain global visual and its corresponding text features \mathbf{F}_v and

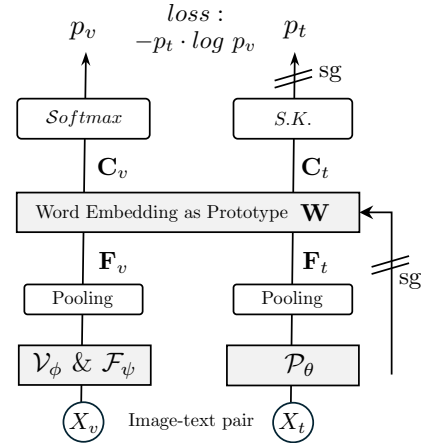


Figure 3. **Alignment Loss.** We illustrate it in the case of one single pair of global vision and text features \mathbf{F}_v and \mathbf{F}_t for simplicity. \mathbf{F}_v and \mathbf{F}_t are mapped by frozen learned prototype \mathbf{W} , i.e., the word embedding of LLMs. Then, they are converted into normalized probabilities using the Softmax function and iterative Sinkhorn-Knopp algorithm [12], respectively. Then, cross-entropy is applied as the loss. To prevent information leakage, the text features are extracted without image prefixes.

$\mathbf{F}_t \in \mathbb{R}^{B \times D_t}$ through the VFM and LLM by parameter-free global average pooling, respectively, as follows:

$$\mathbf{F}_v = \text{Pool}(\mathbf{H}_v), \mathbf{F}_t = \text{Pool}(\mathcal{P}_\theta(X_t)) \quad (7)$$

where B denotes the mini-batch size, D_t represents the hidden dimension of LLM and X_t is a piece of corresponding text to \mathbf{H}_v . And then, we map \mathbf{F}_v , \mathbf{F}_t into language space by the prototype $\mathbf{W} \in \mathbb{R}^{D_t \times K}$ as follows:

$$\mathbf{C}_v = \mathbf{W}^\top \mathbf{F}_v, \mathbf{C}_t = \mathbf{W}^\top \mathbf{F}_t \quad (8)$$

where K indicates the vocabulary size of LLM. To prevent information leakage during training, the text features are extracted without image prefixes. Additionally, we detach the gradient of the word embedding to avoid training collapse.

Model	#PT	#IT	Text-rich and Fine-grained				General and Real-world					
			ChartQA	DocVQA [†]	AI2D	Inst-IT	VQAv2	GQA	MMMU [†]	MMBench [†]	RWQA	
<i>~1B models</i>												
Deepseek-VL [45]	3.75M	N/A	-	-	51.5	-	-	-	32.2	-	-	-
LLaVA-OV (SI) [32]	4.6M	3.2M	61.0	75.0	54.2	44.2	-	-	31.2	43.8	53.7	
LLaVA-OV [32]	4.6M	4.8M	61.4	73.7	57.1	47.8	-	-	31.4	52.1	55.6	
COMP-MM	4.6M	3.2M	66.7	75.9	61.9	50.1	78.2	60.4	33.0	56.4	58.3	
<i>~7B models</i>												
LLaVA-1.5 [40]	558K	665K	18.2	28.1	-	32.1	78.5	62.0	35.3	-	-	
LLaVA-NeXT [43]	558K	765K	54.8	74.4	-	42.4	81.8	64.2	35.1	-	-	
Deepseek-VL [45]	3.75M	N/A	-	-	65.3	-	-	-	36.6	-	-	
Cambrian-1 [65]	1.2M	7.0M	73.3	77.8	73.0	-	-	64.6	42.7	-	64.2	
LLaVA-OV (SI) [32]	4.6M	3.2M	78.8	89.3	81.6	61.8	-	-	47.3	81.7	65.5	
LLaVA-OV [32]	4.6M	4.8M	80.0	90.2	81.4	71.7	-	-	48.8	80.8	66.3	
COMP-MM	4.6M	3.2M	<u>79.6</u>	91.0	81.4	<u>65.0</u>	81.9	65.9	48.9	<u>81.4</u>	66.4	

Table 1. **Main results of COMP-MM on multimodal understanding benchmarks.** #PT indicates the size of pre-training dataset. #IT indicates the size of instruction tuning dataset. N/A indicates the size is unknown. [†] denotes we report the performance on validation sets.

Moreover, for adapting the learned prototype, we replace the Softmax function, which assumes a uniform distribution, with the Sinkhorn-Knopp algorithm [12] that explores the prior distribution of word embeddings [52] to obtain soft normalized probabilities of \mathbf{C}_t :

$$p_t = \text{Diag}(\mathbf{u}_W) \exp\left(\frac{\mathbf{C}_t}{\epsilon}\right) \text{Diag}(\mathbf{v}) \quad (9)$$

where $\mathbf{u}_W \in \mathbb{R}^K$ is the prior marginal distribution of words, and $\mathbf{v} \in \mathbb{R}^B$ are renormalization vectors. Thus, the alignment loss can be formally expressed as:

$$L_{align} = -p_t \cdot \log p_v \quad (10)$$

where, $p_v = \text{Softmax}(\mathbf{C}_v)$. Additionally, we stop the gradient propagation for LLM, ensuring that L_{align} updates only the parameters of VFM.

3.4. Training Recipe

Our continual pre-training is divided into three stages:

- **Stage-I: Vision-language adapter warming up.** In this stage, we freeze the VFM and the LLM, and only train the adapter at fixed low image resolution without RoPE-2D.
- **Stage-II: Native resolution adaptation.** In this stage, we train the entire model with RoPE-2D a piece of time at fixed high image resolution, followed by another piece of time at native resolution.
- **Stage-III: Instruction tuning (optional).** In this stage, we fine-tune the entire model on the instruction dataset at native resolution with RoPE-2D, to accommodate different types of data inputs.

The training objective can be formally expressed as:

$$\mathcal{L} = \begin{cases} L_{dec} + \alpha \cdot L_{align} & \text{in Stage-I \& II} \\ L_{dec} & \text{in Stage-III} \end{cases} \quad (11)$$

where α is loss weight to balance L_{dec} and L_{align} .

4. Experiments

All experiments are conducted on two strong mainstream VFs, SigLIP [80] and DINOv2 [50], to verify the applicability of our method across models with different pre-training objectives. We evaluated the performance of our COMP-MM on multimodal benchmarks with other LMs. Additionally, we conducted detailed comparisons with other VFs across various visual downstream tasks, including multimodal understanding, image classification, and semantic segmentation.

4.1. COMP-MM

Setup. We utilize SigLIP-So400M [80] as pre-trained VF and Qwen2.5-0.5B, Qwen2.5-7B [77] as pre-trained LLM, and the cross-modality adapter is a 2x2 downsampling MLP. For Stage-I, we train the adapter on LLaVA-Pretrain data [41] at 384px resolution. For Stage-II, we train the full model on LLaVA-Mid-Stage data [32] at 1024px and native resolution. To support high resolution inputs, we replace 1M data in CC3M [61] with Densefusion-1M [36]. For Stage-III, we train the full model on LLaVA-OV-SI SFT data [32] at native resolution. All experiments are conducted on $8 \times H100$.

Results. As shown in Tab. 1, under the similar pre-training data size, our model significantly outperforms all other

Model	ViT	#Patches	OKVQA [†]	TextVQA [†]	DocVQA	InfoVQA	ChartQA	SEED	MME
DINOv2 [50]	L/14	576	54.1	13.4	7.3	21.3	10.8	57.0	1345
DINOv2 [50]	G/14	3034	56.9	15.1	8.2	19.7	12.0	68.9	1423
CLIP [57]	L/14	576	60.0	47.5	25.6	21.8	19.2	70.1	1481
SigLIP [80]	L/14	576	59.3	44.1	16.9	20.7	14.4	66.8	1416
SigLIP [80]	So/14	729	60.1	47.5	19.2	21.0	14.7	67.5	1433
AIMv2 [20]	L/14	576	60.8	53.6	26.6	22.8	19.2	71.8	1472
AIMv2 [20]	H/14	576	61.3	<u>55.5</u>	<u>27.8</u>	<u>23.1</u>	19.9	72.1	1545
CoMP-DINOv2	L/14	576	59.0	53.6	24.7	22.8	<u>23.8</u>	<u>72.8</u>	1484
CoMP-SigLIP	So/14	576	<u>61.0</u>	62.5	34.0	26.0	25.0	74.3	<u>1543</u>

Table 2. **Evaluation on multimodal understanding benchmarks.** We conduct extensive experiments on CoMP-SigLIP and CoMP-DINOv2 with LLaMA-3.0 8B [19], freezing the vision encoder and directly tuning on LLaVA SFT data [41] for one epoch. #Patches indicates the number of input visual patches for the LLM. [†] denotes we report the performance on validation sets.

methods and achieves state-of-the-art performance among open-source models across multiple benchmarks and on both 1B models and 7B models. Specifically, CoMP outperforms LLaVA-OV-SI [32], a strong baseline that employs the AnyRes technique for high-resolution input, not only on text-rich and fine-grained understanding tasks such as ChartQA [57], DocVQA [47], AI2D [28], and InstIT [53], but also on various general and real-world multimodal understanding tasks like VQAv2 [23], GQA [26], MMMU [79], MMBench [44] and RealWorldQA [73].

Model	ViT	Pre-training Res.	224px	448px
AIMv2 [20]	L/14	224px	86.6	84.8
AIMv2 [20]	L/14	448px	78.9	87.9
AIMv2 [20]	L/14	Native	86.1	87.1
MAE [25]	H/14	224px	78.5	-
DINOv2 [50]	L/14	224→518px	86.3	87.6
CoMP-DINOv2	L/14	Native	<u>85.7</u>	<u>86.5</u>
CLIP [57]	L/14	224→336px	84.4	83.8
SigLIP [80]	So/14	224→384px	87.1	88.2
LLaVA-SigLIP [32]	So/14	224→384px	83.2	84.4
CoMP-SigLIP	So/14	Native	86.5	87.4

Table 3. **Evaluation on frozen trunk classification.** All experiments are conducted on ImageNet-1K [16] at 224px and 448px by utilizing attentive pooling probing.

4.2. Multimodal Understanding

Setup. To further quantify the performance of CoMP for LMMs, we compare it with other mainstream VFM following the settings and hyperparameters in [20]. Specifically, we reinitialize an adapter between CoMP vision encoder and LLM, *e.g.* LLaMA 3.0 8B [19], and freeze the parame-

ters of vision encoder all the time. We train the adapter and the LLM jointly in a single stage on LLaVA SFT data [41] for one epoch, and scale up the learning rate of adapter by a factor of 8. To ensure fairness, we used the checkpoint before instructing tuning (Stage III) to confirm that the model had not been exposed to instruction tuning data and fixed the number of patches input to the LLM at 576.

Results. We evaluate CoMP across various benchmarks covering general knowledge (OKVQA [60], SEED-Bench [31], MME [21]) and text-rich (TextVQA [62], DocVQA [47], InfoVQA [48], ChartVQA [46]) tasks. As presented in Tab. 2, our models outperform CLIP, SigLIP and DINOv2 by a significant margin. Notably, our CoMP-SigLIP-400M outperforms AIMv2-H (600M) on most tasks, and our CoMP-DINOv2-L also surpasses DINOv2-G, demonstrating the effectiveness of our CoMP.

Model	ViT	504px	672px
InternViT-v2.5 [11]	6B	55.4	53.9
DINOv2 [50]	L/14	55.3	55.9
CoMP-DINOv2	L/14	52.7	53.0
SigLIP [80]	So/14	35.2	31.6
SigLIP 2 (NaFlex) [68]	So/16	35.3	34.8
LLaVA-SigLIP [32]	So/14	39.9	36.5
CoMP-SigLIP	So/14	49.5	49.1

Table 4. **Evaluation on semantic segmentation.** All experiments are conducted on ADE20K [82] at 504px and 672px by freezing the backbone and only train the UperNet [74] head.

4.3. Image Recognition

Setup. We evaluate the global-view semantic quality of CoMP by image classification on ImageNet-1K [16]. In detail, we utilize attentive pooling probing, *i.e.* adding an

#		AI2D	ChartQA	DocVQA	Δ
1	Baseline Recipe	50.2	29.9	24.1	-
2	+ RoPE-2D from Stage-I†	51.5	11.0	11.4	↓ 10.1
3	+ RoPE-2D from Stage-II	55.4	56.9	61.6	↑ 23.2
4	+ Freezing LM in Stage-II	54.6	55.4	55.3	↓ 2.87
5	+ Native Resolution Training	56.7	59.5	67.7	↑ 3.33
6	+ Increase Resolution to 1024px in Stage-II	56.2	59.9	68.8	↑ 0.33
7	+ Scale Up Training Data	62.0	65.2	75.0	↑ 5.77
8	+ Alignment Loss	61.9	66.7	75.9	↑ 0.77
9	Replace with DINOv2-Large in #7	58.9	61.5	68.5	-
10	+ Alignment Loss	59.6	64.0	70.1	↑ 1.60

Table 5. **Ablation on training recipe.** The first row presents the baseline three-stage training recipe, with progressive resolutions of 384px, 576px, and 768px. In the first stage, only the adapter is unfrozen, while in the subsequent stages, the full model is fine-tuned. Each following row modifies strategy from the last non-italicized row, and our final recipe is highlighted in blue. Experiments are run using SigLIP-400M and Qwen2.5-0.5B. †: Unfreezing vision encoder for RoPE training; Δ : The average of the difference from previous row.

attention pooling layer on top of the frozen features, to train our method at fixed 224px and 448px. To further analyze the recognition performance of our model, we evaluate a SigLIP variant from the checkpoint of LLaVA-OV-SI-0.5B model, denoting it as LLaVA-SigLIP. All our vision models are from Stage-II of CoMP-MM-1B.

Results. As shown in 3, our model preserves the rich global features of the original SigLIP and DINOv2 while supporting native resolution inputs, and the CoMP-SigLIP surpasses the native resolution version of AIMv2. Notably, our CoMP-SigLIP also outperforms LLaVA-SigLIP from LLaVA-OV-SI-0.5B checkpoint by a large margin, indicating our approach can better preserve the classification ability after the continual pretraining.

4.4. Semantic Segmentation

Setup. We evaluate the local-view semantic quality of CoMP semantic segmentation on ADE20K [82], utilizing UperNet [74] by head tuning. Specifically, we freeze the backbone and only train the UperNet head at fixed 504px and 672px. To further analyze the segmentation performance of our model, we evaluate SigLIP 2 NaFlex variant [68], which also supports native resolution inputs, and LLaVA-SigLIP which is from the checkpoint of LLaVA-OV-SI-0.5B model. All our vision models are from Stage-II of CoMP-MM-1B.

Results. As shown in Tab. 4, for vision-only pre-training DINOv2, which excels at extracting dense features, our continual multimodal pre-training effectively preserves the semantic segmentation capability; for vision-language pre-training SigLIP, which suffers from extracting local feature, CoMP significantly enhances its pixel-level understanding ability with a great margin.

4.5. Ablation Study

Improved Training Recipe. Tab. 5 presents the roadmap from the commonly used LLaVA-1.5-like architecture to our proposed CoMP. Specifically, we begin our experiments with a data combination strategy basically following LLaVA-OV [32]. This setup includes LCS-558K in Stage I for initializing the projection module, approximately 4M recaptioned data in the middle stage for high-quality knowledge learning, and around 0.8M single-image instruction-tuning data from LLaVA-Next [43]. During the first stage, only the adapter is unfrozen, while in the subsequent stages, the full model undergoes fine-tuning.

We adopt SigLIP-So400M [80] as the vision encoder and Qwen2.5-0.5B [77] as the language decoder. Additionally, we progressively increase the input resolution across stages, using 384px, 576px, and 768px, respectively, by interpolation to the fixed-size position embeddings. As shown in line #1 of Tab. 5, the baseline model struggles with tasks such as ChartQA and DocVQA, which involve high-resolution images and require fine-grained visual understanding.

To support native resolution, we explore integrating ROPE-2D while retaining the original fixed-size position embeddings. However, adding ROPE-2D in the first stage leads to training collapse, likely due to the frozen vision transformer struggling to adapt to ROPE-2D, resulting in unstable optimization. In contrast to the previous works [71] that freeze the language model before the instruction tuning stage, we find it is necessary to unlock the language model for better multimodal pertaining, refer to line#4. Building on effective high-resolution pretraining, we introduce an additional round of dynamic resolution pre-training in Stage 2, adjusting to the native resolution of visual inputs. This strategy consistently enhances performance across various benchmarks.

P.E.	Res.	ChartQA	DocVQA
Learned P.E.	384px	22.8	24.3
Learned P.E.	768px	28.8	29.9
RoPE-2D	768px	8.24	11.9
C-ROPE	768px	32.2	33.2

Table 6. **Ablation on positional embeddings.** We utilize Qwen2-0.5B [76] and SigLIP-400M [80] to be directly fine-tuned on LLaVA-NeXT-SFT [43] data for one epoch.

Additionally, as shown in line #9, replacing SigLIP with DINOv2-L results in a slight performance drop. However, when alignment loss is incorporated, the model achieves performance comparable to that of vision-language pre-training models. This suggests that feature alignment objectives are particularly crucial for vision-only models that do not undergo explicit vision-language pretraining.

Effectiveness of C-ROPE. We utilize Qwen2-0.5B [76] and SigLIP-400M [80] to directly fine-tune on LLaVA-NeXT-SFT data [43] for one epoch in three different settings: (1) Only learned position embedding with interpolation at pre-trained resolution 384px and higher resolution 768px, (2) only RoPE-2D and directly removing original position embedding [71] at 768px, and (3) C-ROPE at 768px. As shown in Tab. 6, although the learned position embedding can obtain a certain capability to process high-resolution inputs through interpolation, C-ROPE can further unleash the performance by a large margin. Moreover, the performance degradation observed when directly using RoPE-2D, suggests that it is neither a data-efficient nor a training-friendly approach, which is due to the removal of traditional position embeddings and the introduction of abrupt changes compared to the pre-trained model.

Effectiveness of Alignment Loss. To further evaluate the effectiveness of Alignment Loss, we utilize Qwen2.5-0.5B [76] and DINOv2-Large [50], and replace the training data of Stage-III with LLaVA-NeXT-SFT data [43] for rapid evaluation in three different settings: (1) without Alignment Loss, (2) with Alignment Loss when the inputs are fixed resolution in Stage-I, II and (3) with Alignment Loss during entire Stage-I, II, including native resolution training. As shown in Tab. 7, Alignment Loss is particularly beneficial for text-rich tasks, and generally, the longer it is applied, the better the performance. Therefore, we use Alignment Loss in both entire Stage I and Stage II by default.

Comparisons with Different VFM. As shown in Tab. 8, we explore different VFM with SigLIP-Base, SigLIP-400M and DINOv2-Large. The results demonstrate that our method is applicable not only to different pre-training objectives (SigLIP vs DINOv2) but also to various model sizes (Base vs Large).

Recipe	ChartQA	DocVQA	MMMU
No Alignment loss	55.6	60.9	31.9
Only fixed res.	59.6	68.4	31.8
Both fixed & native res.	60.2	67.5	32.9

Table 7. **Ablation on the effectiveness of Alignment loss.** We utilize Qwen2-0.5B [76] and DINOv2-Large [50], and employ LLaVA-NeXT-SFT [43] as training data of Stage-III.

Model	ChartQA	DocVQA	MMMU
SigLIP-Base [80]	61.6	71.0	33.6
SigLIP-So400M [80]	66.7	75.9	33.0
DINOv2-Large [50]	64.0	70.1	32.2

Table 8. **Ablation on vision encoders.** We ablation the vision encoder of different model sizes and pretraining tasks.

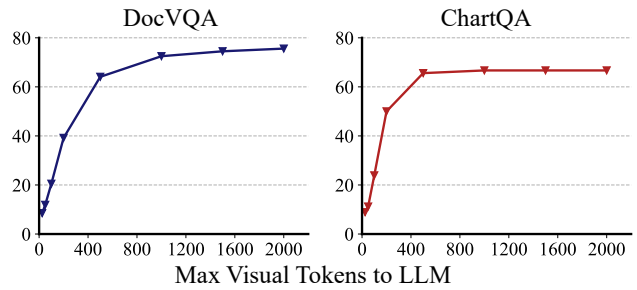


Figure 4. **Varying the image resolution during inference.** We investigate the impact of image resolution on DocVQA [47] and ChartQA [46] by our COMP-MM-1B.

Varying the Resolution during Inference. To investigate the impact of image resolution on resolution-sensitive tasks, we observe the changes in scores on DocVQA [47] and ChartQA [46] by limiting the max number of visual tokens to LLM. As shown in Fig. 4, as the input resolution increases, the performance of both tasks gradually improves, which demonstrates the effectiveness of our approach for varying resolutions, particularly the high resolution.

5. Conclusion

We introduced COMP, a continual multimodal pre-training pipeline to tackle fixed resolution and modality gap problems under LMM framework, for both vision-language pre-training and vision-only pre-training models. Specifically, we proposed C-ROPE and Alignment Loss, which efficiently adapt to native resolution inputs with light continual training data and are better suited for the LLM text space. Through extensive experiments, we demonstrated that our approach achieved state-of-the-art performance on multi-modal understanding benchmarks, and the performance of the VFM in other downstream visual tasks is preserved.

References

- [1] Pravesh Agrawal, Szymon Antoniak, Emma Bou Hanna, Baptiste Bout, Devendra Chaplot, Jessica Chudnovsky, Diogo Costa, Baudouin De Moncault, Saurabh Garg, Theophile Gervet, Soham Ghosh, Amélie Héliou, Paul Jacob, Albert Q. Jiang, Kartik Khandelwal, Timothée Lacroix, Guillaume Lample, Diego Las Casas, Thibaut Lavril, Teven Le Scao, Andy Lo, William Marshall, Louis Martin, Arthur Mensch, Pavankumar Muddireddy, Valera Nemychnikova, Marie Pellat, Patrick Von Platen, Nikhil Raghuraman, Baptiste Rozière, Alexandre Sablayrolles, Lucile Saulnier, Romain Sauvestre, Wendy Shang, Roman Soletskyi, Lawrence Stewart, Pierre Stock, Joachim Studnia, Sandeep Subramanian, Sagar Vaze, Thomas Wang, and Sophia Yang. Pixtral 12b. *arXiv preprint arXiv:2410.07073*, 2024. 3
- [2] Jean-Baptiste Alayrac, Jeff Donahue, Pauline Luc, Antoine Miech, Iain Barr, Yana Hasson, Karel Lenc, Arthur Mensch, Katherine Millican, Malcolm Reynolds, et al. Flamingo: a visual language model for few-shot learning. *NeurIPS*, 2022. 3
- [3] Jinze Bai, Shuai Bai, Yunfei Chu, Zeyu Cui, Kai Dang, et al. Qwen Technical Report. *arXiv preprint arXiv:2309.12345*, 2023. 2
- [4] Jinze Bai, Shuai Bai, Shusheng Yang, Shijie Wang, Sinan Tan, Peng Wang, Junyang Lin, Chang Zhou, and Jingren Zhou. Qwen-vl: A frontier large vision-language model with versatile abilities. *arXiv preprint arXiv:2308.12966*, 2023. 3
- [5] Shuai Bai, Keqin Chen, Xuejing Liu, Jialin Wang, Wenbin Ge, Sibo Song, Kai Dang, Peng Wang, Shijie Wang, Jun Tang, Humen Zhong, Yuanzhi Zhu, Mingkun Yang, Zhao-hai Li, Jianqiang Wan, Pengfei Wang, Wei Ding, Zheren Fu, Yiheng Xu, Jiabo Ye, Xi Zhang, Tianbao Xie, Zesen Cheng, Hang Zhang, Zhibo Yang, Haiyang Xu, and Junyang Lin. Qwen2.5-vl technical report. *arXiv preprint arXiv:2502.13923*, 2025. 3
- [6] Hangbo Bao, Li Dong, Songhao Piao, and Furu Wei. Beit: Bert pre-training of image transformers. In *ICLR*, 2021. 2
- [7] Lucas Beyer, Pavel Izmailov, Alexander Kolesnikov, Mathilde Caron, Simon Kornblith, Xiaohua Zhai, Matthias Minderer, Michael Tschannen, Ibrahim Alabdulmohsin, and Filip Pavetic. Flexivit: One model for all patch sizes. In *CVPR*, 2023. 2, 3
- [8] Tom Brown, Benjamin Mann, Nick Ryder, Melanie Subbiah, Jared D Kaplan, Prafulla Dhariwal, Arvind Neelakantan, Pranav Shyam, Girish Sastry, Amanda Askell, et al. Language models are few-shot learners. *NeurIPS*, 2020. 2, 3
- [9] Mathilde Caron, Hugo Touvron, Ishan Misra, Hervé Jégou, Julien Mairal, Piotr Bojanowski, and Armand Joulin. Emerging properties in self-supervised vision transformers. In *CVPR*, 2021. 1, 2, 4
- [10] Ting Chen, Simon Kornblith, Mohammad Norouzi, and Geoffrey Hinton. A simple framework for contrastive learning of visual representations. In *ICML*, 2020. 1, 2
- [11] Zhe Chen, Weiyun Wang, Yue Cao, Yangzhou Liu, Zhangwei Gao, Erfei Cui, Jinguo Zhu, Shenglong Ye, Hao Tian, Zhaoyang Liu, Lixin Gu, Xuehui Wang, Qingyun Li, Yimin Ren, Zixuan Chen, Jiapeng Luo, Jiahao Wang, Tan Jiang, Bo Wang, Conghui He, Botian Shi, Xingcheng Zhang, Han Lv, Yi Wang, Wenqi Shao, Pei Chu, Zhongying Tu, Tong He, Zhiyong Wu, Huipeng Deng, Jiaye Ge, Kai Chen, Kaipeng Zhang, Limin Wang, Min Dou, Lewei Lu, Xizhou Zhu, Tong Lu, Dahua Lin, Yu Qiao, Jifeng Dai, and Wenhui Wang. Expanding performance boundaries of open-source multi-modal models with model, data, and test-time scaling. *arXiv preprint arXiv:2412.05271*, 2025. 3, 6
- [12] Marco Cuturi. Sinkhorn distances: Lightspeed computation of optimal transport. In *NeurIPS*, 2013. 4, 5
- [13] Wenliang Dai, Junnan Li, Dongxu Li, Anthony Meng Huat Tiong, Junqi Zhao, Weisheng Wang, Boyang Li, Pascale N Fung, and Steven Hoi. Instructblip: Towards general-purpose vision-language models with instruction tuning. *NeurIPS*, 2024. 3
- [14] DeepSeek-AI, Aixin Liu, Bei Feng, Bing Xue, Bingxuan Wang, Bochao Wu, Chengda Lu, Chenggang Zhao, Chengqi Deng, Chenyu Zhang, Chong Ruan, Damai Dai, Daya Guo, Dejian Yang, Deli Chen, Dongjie Ji, Erhang Li, Fangyun Lin, Fucong Dai, Fuli Luo, Guangbo Hao, Guanting Chen, Guowei Li, H. Zhang, Han Bao, Hanwei Xu, Haocheng Wang, Haowei Zhang, Honghui Ding, Huajian Xin, Huazuo Gao, Hui Li, Hui Qu, J. Zhang, et al. Deepseek-v3 technical report. *arXiv preprint arXiv:2412.19437*, 2024. 2
- [15] Mostafa Dehghani, Basil Mustafa, Josip Djolonga, Jonathan Heek, Matthias Minderer, Mathilde Caron, Andreas Steiner, Joan Puigcerver, Robert Geirhos, Ibrahim M Alabdulmohsin, et al. Patch n'pack: Navit, a vision transformer for any aspect ratio and resolution. In *NeurIPS*, 2023. 3
- [16] Jia Deng, Wei Dong, Richard Socher, Li-Jia Li, Kai Li, and Li Fei-Fei. Imagenet: A large-scale hierarchical image database. In *CVPR*, 2009. 6, 13
- [17] Jacob Devlin, Ming-Wei Chang, Kenton Lee, and Kristina Toutanova. Bert: Pre-training of deep bidirectional transformers for language understanding. *arXiv preprint arXiv:1810.04805*, 2018. 2
- [18] Alexey Dosovitskiy, Lucas Beyer, Alexander Kolesnikov, Dirk Weissenborn, Xiaohua Zhai, Thomas Unterthiner, Mostafa Dehghani, Matthias Minderer, Georg Heigold, Sylvain Gelly, Jakob Uszkoreit, and Neil Houlsby. An image is worth 16x16 words: Transformers for image recognition at scale. In *ICLR*, 2021. 2
- [19] Avijit Dubey, Aaron Grattafiori, et al. The llama 3 herd of models. *arXiv preprint arXiv:2407.21783*, 2024. 2, 6, 13
- [20] Enrico Fini, Mustafa Shukor, Xiujun Li, Philipp Dufter, Michal Klein, David Halldmann, Sai Aitharaju, Victor Guilherme Turrisi da Costa, Louis Béthune, Zhe Gan, Alexander T Toshev, Marcin Eichner, Moin Nabi, Yinfei Yang, Joshua M. Susskind, and Alaaddin El-Nouby. Multimodal autoregressive pre-training of large vision encoders. *arXiv preprint arXiv:2411.14402*, 2024. 6
- [21] Chaoyou Fu, Peixian Chen, Yunhang Shen, Yulei Qin, Mengdan Zhang, Xu Lin, Jinrui Yang, Xiawu Zheng, Ke Li, Xing Sun, et al. Mme: A comprehensive evaluation benchmark for multimodal large language models. *arXiv preprint arXiv:2306.13394*, 2023. 6

- [22] Peng Gao, Renrui Zhang, Chris Liu, Longtian Qiu, Siyuan Huang, Weifeng Lin, Shitian Zhao, Shijie Geng, Ziyi Lin, Peng Jin, et al. Sphinx-x: Scaling data and parameters for a family of multi-modal large language models. *arXiv preprint arXiv:2402.05935*, 2024. 3
- [23] Yash Goyal, Tejas Khot, Douglas Summers-Stay, Dhruv Batra, and Devi Parikh. Making the v in vqa matter: Elevating the role of image understanding in visual question answering. In *CVPR*, 2017. 6
- [24] Kaiming He, Haoqi Fan, Yuxin Wu, Saining Xie, and Ross Girshick. Momentum contrast for unsupervised visual representation learning. In *CVPR*, 2020. 1, 2
- [25] Kaiming He, Xinlei Chen, Saining Xie, Yanghao Li, Piotr Dollár, and Ross Girshick. Masked autoencoders are scalable vision learners. In *CVPR*, 2022. 2, 6
- [26] Drew A Hudson and Christopher D Manning. Gqa: A new dataset for real-world visual reasoning and compositional question answering. In *CVPR*, 2019. 6
- [27] Chao Jia, Yinfai Yang, Ye Xia, Yi-Ting Chen, Zarana Parekh, Hieu Pham, Quoc Le, Yun-Hsuan Sung, Zhen Li, and Tom Duerig. Scaling Up Visual and Vision-Language Representation Learning With Noisy Text Supervision. In *ICML*, 2021. 3
- [28] Aniruddha Kembhavi, Mike Salvato, Eric Kolve, Minjoon Seo, Hannaneh Hajishirzi, and Ali Farhadi. A diagram is worth a dozen images. In *ECCV*, 2016. 6
- [29] Zhenzhong Lan, Mingda Chen, Sebastian Goodman, Kevin Gimpel, Piyush Sharma, and Radu Soricut. Albert: A lite bert for self-supervised learning of language representations. *arXiv preprint arXiv:1909.11942*, 2019. 2
- [30] Mike Lewis, Yinhan Liu, Naman Goyal, Marjan Ghazvininejad, Abdelrahman Mohamed, Omer Levy, Ves Stoyanov, and Luke Zettlemoyer. Bart: Denoising sequence-to-sequence pre-training for natural language generation, translation, and comprehension. *arXiv preprint arXiv:1910.13461*, 2019. 2
- [31] Bohao Li, Rui Wang, Guangzhi Wang, Yuying Ge, Yixiao Ge, and Ying Shan. Seed-bench: Benchmarking multimodal llms with generative comprehension. *arXiv preprint arXiv:2307.16125*, 2023. 6
- [32] Bo Li, Yuanhan Zhang, Dong Guo, Renrui Zhang, Feng Li, Hao Zhang, Kaichen Zhang, Peiyuan Zhang, Yanwei Li, Ziwei Liu, and Chunyuan Li. Llava-onevision: Easy visual task transfer. *TMLR*, 2024. 2, 5, 6, 7, 13
- [33] Junnan Li, Dongxu Li, Caiming Xiong, and Steven Hoi. Blip: Bootstrapping language-image pre-training for unified vision-language understanding and generation. In *ICML*, 2022. 3
- [34] Junnan Li, Dongxu Li, Silvio Savarese, and Steven Hoi. Blip-2: Bootstrapping language-image pre-training with frozen image encoders and large language models. In *ICML*, 2023. 3
- [35] Junnan Li, Dongxu Li, Silvio Savarese, and Steven C. H. Hoi. Blip-2: Bootstrapping language-image pre-training with frozen image encoders and large language models. In *ICML*, 2023. 3
- [36] Xiaotong Li, Fan Zhang, Haiwen Diao, Yueze Wang, Xinlong Wang, and Ling-Yu Duan. Densefusion-1m: Merging vision experts for comprehensive multimodal perception. In *NeurIPS*, 2024. 5
- [37] Victor Weixin Liang, Yuhui Zhang, Yongchan Kwon, Serena Yeung, and James Y Zou. Mind the gap: Understanding the modality gap in multi-modal contrastive representation learning. In *NeurIPS*, 2022. 2
- [38] Ji Lin, Hongxu Yin, Wei Ping, Yao Lu, Pavlo Molchanov, Andrew Tao, Huizi Mao, Jan Kautz, Mohammad Shoeybi, and Song Han. Vila: On pre-training for visual language models. *arXiv preprint arXiv:2312.07533*, 2023. 3
- [39] Ziyi Lin, Chris Liu, Renrui Zhang, Peng Gao, Longtian Qiu, Han Xiao, Han Qiu, Chen Lin, Wenqi Shao, Keqin Chen, et al. Sphinx: The joint mixing of weights, tasks, and visual embeddings for multi-modal large language models. *arXiv preprint arXiv:2311.07575*, 2023. 3
- [40] Haotian Liu, Chunyuan Li, Yuheng Li, and Yong Jae Lee. Improved baselines with visual instruction tuning. *ArXiv*, abs/2310.03744, 2023. 3, 5
- [41] Haotian Liu, Chunyuan Li, Qingyang Wu, and Yong Jae Lee. Visual instruction tuning. In *NeurIPS*, 2023. 2, 3, 5, 6
- [42] Haotian Liu, Chunyuan Li, Yuheng Li, Bo Li, Yuanhan Zhang, Sheng Shen, and Yong Jae Lee. Llava-next: Improved reasoning, ocr, and world knowledge, 2024. 13
- [43] Haotian Liu, Chunyuan Li, Yuheng Li, Bo Li, Yuanhan Zhang, Sheng Shen, and Yong Jae Lee. Llava-next: Improved reasoning, ocr, and world knowledge, 2024. 2, 3, 5, 7, 8
- [44] Yuan Liu, Haodong Duan, Yuanhan Zhang, Bo Li, Songyang Zhang, Wangbo Zhao, Yike Yuan, Jiaqi Wang, Conghui He, Ziwei Liu, et al. Mmbench: Is your multi-modal model an all-around player? In *ECCV*, 2024. 6
- [45] Haoyu Lu, Wen Liu, Bo Zhang, Bingxuan Wang, Kai Dong, Bo Liu, Jingxiang Sun, Tongzheng Ren, Zhuoshu Li, Hao Yang, Yaofeng Sun, Chengqi Deng, Hanwei Xu, Zhenda Xie, and Chong Ruan. Deepseek-vl: Towards real-world vision-language understanding. *arXiv preprint arXiv:2403.05525*, 2024. 5
- [46] Ahmed Masry, Xuan Long Do, Jia Qing Tan, Shafiq Joty, and Enamul Hoque. Chartqa: A benchmark for question answering about charts with visual and logical reasoning. In *ACL Findings*, 2022. 2, 6, 8
- [47] Minesh Mathew, Dimosthenis Karatzas, and CV Jawahar. Docvqa: A dataset for vqa on document images. In *WACV*, 2021. 2, 6, 8
- [48] Minesh Mathew, Viraj Bagal, Rubèn Tito, Dimosthenis Karatzas, Ernest Valveny, and CV Jawahar. Infographicvqa. In *WACV*, 2022. 6
- [49] Lingchen Meng, Jianwei Yang, Rui Tian, Xiyang Dai, Zuxuan Wu, Jianfeng Gao, and Yu-Gang Jiang. Deepstack: Deeply stacking visual tokens is surprisingly simple and effective for llms. In *NeurIPS*, 2024. 3
- [50] Maxime Oquab, Timothée Darcret, Théo Moutakanni, Huy Vo, Marc Szafraniec, Vasil Khalidov, Pierre Fernandez, Daniel Haziza, Francisco Massa, Alaaeldin El-Nouby, et al. Dinov2: Learning robust visual features without supervision. *TMLR*, 2024. 1, 2, 4, 5, 6, 8, 13

- [51] Long Ouyang, Jeffrey Wu, Xu Jiang, Diogo Almeida, Carroll Wainwright, Pamela Mishkin, Chong Zhang, Sandhini Agarwal, Katarina Slama, Alex Ray, et al. Training language models to follow instructions with human feedback. *NeurIPS*, 2022. 2
- [52] Jungin Park, Jiyoung Lee, and Kwanghoon Sohn. Bridging vision and language spaces with assignment prediction. In *ICLR*, 2024. 2, 4, 5
- [53] Wujian Peng, Lingchen Meng, Yitong Chen, Yiweng Xie, Yang Liu, Tao Gui, Hang Xu, Xipeng Qiu, Zuxuan Wu, and Yu-Gang Jiang. Inst-it: Boosting multimodal instance understanding via explicit visual prompt instruction tuning. *arXiv preprint arXiv:2412.03565*, 2024. 2, 6
- [54] Wujian Peng, Sicheng Xie, Zuyao You, Shiyi Lan, and Zuxuan Wu. Synthesize diagnose and optimize: Towards fine-grained vision-language understanding. In *CVPR*, 2024. 3
- [55] Alec Radford, Karthik Narasimhan, Tim Salimans, Ilya Sutskever, et al. Improving language understanding by generative pre-training. 2018. 2, 3
- [56] Alec Radford, Jeffrey Wu, Rewon Child, David Luan, Dario Amodei, Ilya Sutskever, et al. Language models are unsupervised multitask learners. *OpenAI blog*, 2019. 2, 3
- [57] Alec Radford, Jong Wook Kim, Chris Hallacy, Aditya Ramesh, Gabriel Goh, Sandhini Agarwal, Girish Sastry, Amanda Askell, Pamela Mishkin, Jack Clark, et al. Learning transferable visual models from natural language supervision. In *ICML*, 2021. 1, 2, 3, 6
- [58] Colin Raffel, Noam Shazeer, Adam Roberts, Katherine Lee, Sharan Narang, Michael Matena, Yanqi Zhou, Wei Li, and Peter J Liu. Exploring the limits of transfer learning with a unified text-to-text transformer. *Journal of machine learning research*, 2020. 2
- [59] Christoph Schuhmann, Romain Beaumont, Richard Vencu, Cade W Gordon, Ross Wightman, Mehdi Cherti, Theo Coombes, Aarush Katta, Clayton Mullis, Mitchell Wortsman, Patrick Schramowski, Srivatsa R Kundurthy, Katherine Crowson, Ludwig Schmidt, Robert Kaczmarczyk, and Jenia Jitsev. LAION-5b: An open large-scale dataset for training next generation image-text models. In *NeurIPS*, 2022. 3
- [60] Dustin Schwenk, Apoorv Khandelwal, Christopher Clark, Kenneth Marino, and Roozbeh Mottaghi. A-okvqa: A benchmark for visual question answering using world knowledge. In *ECCV*, 2022. 6
- [61] Piyush Sharma, Nan Ding, Sebastian Goodman, and Radu Soricut. Conceptual captions: A cleaned, hypernymed, image alt-text dataset for automatic image captioning. In *ACL*, 2018. 5
- [62] Amanpreet Singh, Vivek Natarajan, Meet Shah, Yu Jiang, Xinlei Chen, Dhruv Batra, Devi Parikh, and Marcus Rohrbach. Towards vqa models that can read. In *CVPR*, 2019. 6
- [63] Jianlin Su. Transformer upgrade path: 17. insights into multimodal positional encoding, 2024. 2
- [64] Rui Tian, Zuxuan Wu, Qi Dai, Han Hu, Yu Qiao, and Yu-Gang Jiang. Resformer: Scaling vits with multi-resolution training. In *CVPR*, 2023. 2, 3
- [65] Shengbang Tong, Ellis Brown, Penghao Wu, Sanghyun Woo, Manoj Middepogu, Sai Charitha Akula, Jihan Yang, Shusheng Yang, Adithya Iyer, Xichen Pan, Ziteng Wang, Rob Fergus, Yann LeCun, and Saining Xie. Cambrian-1: A fully open, vision-centric exploration of multimodal llms. *arXiv preprint arXiv:2406.16860*, 2024. 2, 5
- [66] Zhan Tong, Yibing Song, Jue Wang, and Limin Wang. Videomae: Masked autoencoders are data-efficient learners for self-supervised video pre-training. *NeurIPS*, 2022. 2
- [67] Hugo Touvron, Thibaut Lavril, Gautier Izacard, Xavier Martinet, Marie-Anne Lachaux, Timothée Lacroix, Baptiste Rozière, Naman Goyal, Eric Hambro, Faisal Azhar, et al. Llama: Open and efficient foundation language models. *arXiv preprint arXiv:2302.13971*, 2023. 2, 3
- [68] Michael Tschannen, Alexey Gritsenko, Xiao Wang, Muhammad Ferjad Naeem, Ibrahim Alabdulmohsin, Nikhil Parthasarathy, Talfan Evans, Lucas Beyer, Ye Xia, Basil Mustafa, Olivier Hénaff, Jeremiah Harmsen, Andreas Steiner, and Xiaohua Zhai. Siglip 2: Multilingual vision-language encoders with improved semantic understanding, localization, and dense features. *arXiv preprint arXiv:2502.14786*, 2025. 1, 2, 6, 7
- [69] Ashish Vaswani, Noam Shazeer, Niki Parmar, Jakob Uszkoreit, Llion Jones, Aidan N Gomez, Łukasz Kaiser, and Illia Polosukhin. Attention is all you need. In *NeurIPS*, 2017. 2
- [70] Junke Wang, Lingchen Meng, Zejia Weng, Bo He, Zuxuan Wu, and Yu-Gang Jiang. To see is to believe: Prompting gpt-4v for better visual instruction tuning. *arXiv preprint arXiv:2311.07574*, 2023. 3
- [71] Peng Wang, Shuai Bai, Sinan Tan, Shijie Wang, Zhihao Fan, Jinze Bai, Keqin Chen, Xuejing Liu, Jialin Wang, Wenbin Ge, Yang Fan, Kai Dang, Mengfei Du, Xuancheng Ren, Rui Men, Dayiheng Liu, Chang Zhou, Jingren Zhou, and Junyang Lin. Qwen2-vl: Enhancing vision-language model's perception of the world at any resolution. *arXiv preprint arXiv:2409.12191*, 2024. 3, 7, 8
- [72] Size Wu, Wenwei Zhang, Lumin Xu, Sheng Jin, Xiangtai Li, Wentao Liu, and Chen Change Loy. Clipself: Vision transformer distills itself for open-vocabulary dense prediction. In *ICLR*, 2024. 3
- [73] xAI Team. Grok-1.5 vision preview, 2024. 6
- [74] Tete Xiao, Yingcheng Liu, Bolei Zhou, Yuning Jiang, and Jian Sun. Unified perceptual parsing for scene understanding. In *ECCV*, 2018. 6, 7
- [75] Wenhan Xiong, Jingyu Liu, Igor Molybog, Hejia Zhang, Prajjwal Bhargava, Rui Hou, Louis Martin, Rashi Rungta, Karthik Abinav Sankararaman, Barlas Oguz, et al. Effective long-context scaling of foundation models. In *NAACL*, 2024. 3
- [76] An Yang, Baosong Yang, Binyuan Hui, Bo Zheng, Bowen Yu, Chang Zhou, Chengpeng Li, Chengyuan Li, Dayiheng Liu, Fei Huang, Guanting Dong, Haoran Wei, Huan Lin, Jialong Tang, Jialin Wang, Jian Yang, Jianhong Tu, Jianwei Zhang, Jianxin Ma, Jianxin Yang, Jin Xu, Jingren Zhou, Jinze Bai, Jinzheng He, Junyang Lin, Kai Dang, Keming Lu, Keqin Chen, Kexin Yang, Mei Li, Mingfeng Xue, Na Ni, Pei Zhang, Peng Wang, Ru Peng, Rui Men, Ruize Gao, Runji Lin, Shijie Wang, Shuai Bai, Sinan Tan, Tianhang Zhu, Tianhao Li, Tianyu Liu, Wenbin Ge, Xiaodong Deng, Xiaohuan

- Zhou, Xingzhang Ren, Xinyu Zhang, Xipin Wei, Xuancheng Ren, Xuejing Liu, Yang Fan, Yang Yao, Yichang Zhang, Yu Wan, Yunfei Chu, Yuqiong Liu, Zeyu Cui, Zhenru Zhang, Zhifang Guo, and Zhihao Fan. Qwen2 technical report. *arXiv preprint arXiv:2407.10671*, 2024. [2](#), [8](#)
- [77] An Yang, Baosong Yang, Beichen Zhang, Binyuan Hui, Bo Zheng, Bowen Yu, Chengyuan Li, Dayiheng Liu, Fei Huang, Haoran Wei, Huan Lin, Jian Yang, Jianhong Tu, Jianwei Zhang, Jianxin Yang, Jiaxi Yang, Jingren Zhou, Junyang Lin, Kai Dang, Keming Lu, Keqin Bao, Kexin Yang, Le Yu, Mei Li, Mingfeng Xue, Pei Zhang, Qin Zhu, Rui Men, Runji Lin, Tianhao Li, Tianyi Tang, Tingyu Xia, Xingzhang Ren, Xuancheng Ren, Yang Fan, Yang Su, Yichang Zhang, Yu Wan, Yuqiong Liu, Zeyu Cui, Zhenru Zhang, and Zihan Qiu. Qwen2.5 technical report. *arXiv preprint arXiv:2412.15115*, 2025. [2](#), [5](#), [7](#)
- [78] Jiahui Yu, Zirui Wang, Vijay Vasudevan, Legg Yeung, Mojtaba Seyedhosseini, and Yonghui Wu. Coca: Contrastive captioners are image-text foundation models. In *Trans. Mach. Learn. Res.*, 2022. [3](#)
- [79] Xiang Yue, Yuansheng Ni, Kai Zhang, Tianyu Zheng, Ruoqi Liu, Ge Zhang, Samuel Stevens, Dongfu Jiang, Weiming Ren, Yuxuan Sun, Cong Wei, Botao Yu, Ruibin Yuan, Renliang Sun, Ming Yin, Boyuan Zheng, Zhenzhu Yang, Yibo Liu, Wenhao Huang, Huan Sun, Yu Su, and Wenhua Chen. Mmmu: A massive multi-discipline multimodal understanding and reasoning benchmark for expert agi. In *CVPR*, 2024. [6](#)
- [80] Xiaohua Zhai, Basil Mustafa, Alexander Kolesnikov, and Lucas Beyer. Sigmoid loss for language image pre-training. In *ICCV*, 2023. [1](#), [2](#), [5](#), [6](#), [7](#), [8](#), [13](#)
- [81] Beichen Zhang, Pan Zhang, Xiaoyi Dong, Yuhang Zang, and Jiaqi Wang. Long-CLIP: Unlocking the Long-Text Capability of CLIP. *arXiv preprint arXiv:2403.15378*, 2024. [3](#)
- [82] Bolei Zhou, Hang Zhao, Xavier Puig, Sanja Fidler, Adela Barriuso, and Antonio Torralba. Scene parsing through ade20k dataset. In *CVPR*, 2017. [6](#), [7](#), [13](#)
- [83] Zhuofan Zong, Bingqi Ma, Dazhong Shen, Guanglu Song, Hao Shao, Dongzhi Jiang, Hongsheng Li, and Yu Liu. Mova: Adapting mixture of vision experts to multimodal context. *arXiv preprint arXiv:2404.13046*, 2024. [2](#)

A. Hyperparameters

CoMP-MM. We outline the optimization hyperparameters used during CoMP-MM continual pre-training in Tab. 9, and the hyperparameters not listed remain consistent with LLaVA-OneVision [32].

	Trainable	Stage-I		Stage-II		Stage-III
		Adapter	Full Model	Fixed	Native	
Batch Size		32×8	32×8	32×8	16×8	
$LR_{Adapter}$		1×10^{-3}	5×10^{-3}	5×10^{-3}	1×10^{-5}	
LR_{VFM}	-		1×10^{-4}	1×10^{-4}	2×10^{-5}	
LR_{LLM}	-		2×10^{-5}	2×10^{-5}	1×10^{-5}	
Epoch		1		1		1

Table 9. Detailed configuration for each training stage of our CoMP-MM-1B and CoMP-MM-7B models.

Besides, $\mathbf{u}_W(k)$ in Eq. (9) is $\frac{N_k}{\sum_i N_i}$, where N_k is the number of the k -th word in Stage-II dataset, α in Eq. (11) is set to 0.05, and all temperature coefficients are 0.005.

Multimodal Understanding. The hyperparameters used for the instruction tuning are detailed in Tab. 10. We tune CoMP-SigLIP and CoMP-DINOv2 with LLama 3.0.8B [19] on LLaVA SFT data [42] for one epoch. In addition, we used a 2×2 downsampling adapter to unleash the high-resolution perception capability of CoMP-SigLIP and CoMP-DINOv2, while keeping the number of tokenens to LLM at 576 for a fair comparison.

Training Config	
Optimizer	AdamW
Decoder peak learning rate	1×10^{-5}
Decoder peak learning rate	1×10^{-5}
Adapter peak learning rate	8×10^{-5}
Minimum learning rate	0
Learning rate schedule	cosine decay
Batch size	128
Iterations	5197
Warmup ratio	0.05
Transformations	PadToSquare, Resize

Table 10. Detailed configuration of CoMP-SigLIP and CoMP-DINOv2 in instruction tuning for multimodal understanding.

Image Recognition. The hyperparameters used for frozen trunk classification on ImageNet-1k [16] are detailed in Tab. 11. The $mean$ and std in Normalization of CoMP-SigLIP and CoMP-DINOv2 are $[(0.5, 0.5, 0.5), (0.5, 0.5, 0.5)]$ and $[(0.485, 0.456, 0.406), (0.229, 0.224, 0.225)]$

respectively, following the original SigLIP [80] and DINOv2 [50]. We use the same hyperaparmeters for all models and baselines.

Training Config	224px	448px
Optimizer	AdamW	
Peak learning rate	1×10^{-4}	1×10^{-5}
Minimum learning rate	2×10^{-5}	5×10^{-6}
Learning rate schedule		cosine decay
Batch size	1024	256
Weight decay		0.05
Epochs		10
Warmup epochs		1
Augmentations:		
RandomResizedCrop		
size	224px	448px
scale		(0.08, 1.0)
ratio		(0.75, 1.33)
interpolation		Bicubic
RandomHorizontalFlip		$p = 0.5$
ToTensor		
Normalize		follows SigLIP or DINOv2

Table 11. Detailed configuration of CoMP-SigLIP and CoMP-DINOv2 for frozen trunk classification.

Semantic Segmentation. The hyperaparmeters used for semantic segmentation on ADE20K [82] are detailed in Tab. 12. The $mean$ and std in Normalization of CoMP-SigLIP and CoMP-DINOv2 follow the original SigLIP [80] and DINOv2 [50].

Training Config	504px	672px
Optimizer	AdamW	
Weight decay		0.05
Peak learning rate		4×10^{-5}
Minimum learning rate		0
Learning rate schedule		poly decay
Batch size		16
Iterations		80K
Warmup iters		1500
Augmentations:		
RandomResizedCrop	504px	672px
RandomFlip		$p = 0.5$
PhotoMetricDistortion		
Normalize		follows SigLIP or DINOv2

Table 12. Detailed configuration of CoMP-SigLIP and CoMP-DINOv2 for semantic segmentation.